Journal of Korean Magnetics Society, Volume 5, Number 5, October 1995

HYBRIDIZATION EFFECTS IN RT_2 COMPOUNDS
(R = Ce, Pr, Nd, Sm, Gd; T = Fe, Co, Ni)

Kicheon Kang and B. I. Min
Department of Physics, Pohang University of Science and Technology
Pohang 790-784, Korea

J. -S. Kang
Research Institute of Industrial Science and Technology
Pohang 790-600, Korea

Employing the muffin-tin-orbital theory combined with pseudo-potential concepts, we have evaluated hybridization matrix elements between R and T sites in RT_2 compounds. The matrix elements are calculated with two parameters, the interatomic distance between R and T atoms from the crystal structure data, and the expectation values of the radial distances for the radial wave functions of the ground state charge densities, which are obtained from the linearized muffin-tin orbital band method within the local density approximation. It is found that the R $4f$ /T $3d$ hybridization matrix elements decrease with an increasing atomic number from R=Ce to Gd, and that they are smaller in RNi_2 than in RCo_2, which are consistent with trends observed in recent photoemission spectroscopy experiments. It is also found that the magnitudes of the hybridization matrix elements in RFe_2 are comparable to those in RNi_2.

I. INTRODUCTION

Recent photoemission spectroscopy (PES) studies for the rare-earth (R) -transition metal (T) compounds [1,2] show that there are non-negligible hybridizations between the R $4f-$ and conduction electrons (R=Ce, Pr, Nd; T=Co, Ni). Figure 1 displays the extracted R $4f$ PES spectra for RNi_2(solid lines) in comparison with those for RCo_2(dashed lines) [2]. Some interesting features are observed in the Fig.1. First, the extracted R $4f$ PES spectra exhibit double-peak structures, one well below the Fermi energy, E_F, and the other near E_F, where the spectral weight near E_F decreases from Ce to Pr and Nd. The peaks well below E_F corresponds to the trivalent R $4f^n \rightarrow 4f^{n-1}$ transitions [3]. The peaks near E_F are known to arise from hybridization effects between R $4f$ and conduction electrons [4–7]. Second, for the Same R, the width of the trivalent peak well below E_F is narrower and the spectral intensity near E_F, relative to that of the trivalent peak, is narrower in RNi_2 than in RCo_2. Finally, the positions of the trivalent peaks, ε_f, (R $4f^n \rightarrow 4f^{n-1}$ transitions) in these compounds are shifted to slightly higher binding energies (about $0.5eV$), as compared to pure rare earth metals [8].

It is speculated that the above features indicate : (i) The R $4f$/T $3d$ hybridization effects decrease from

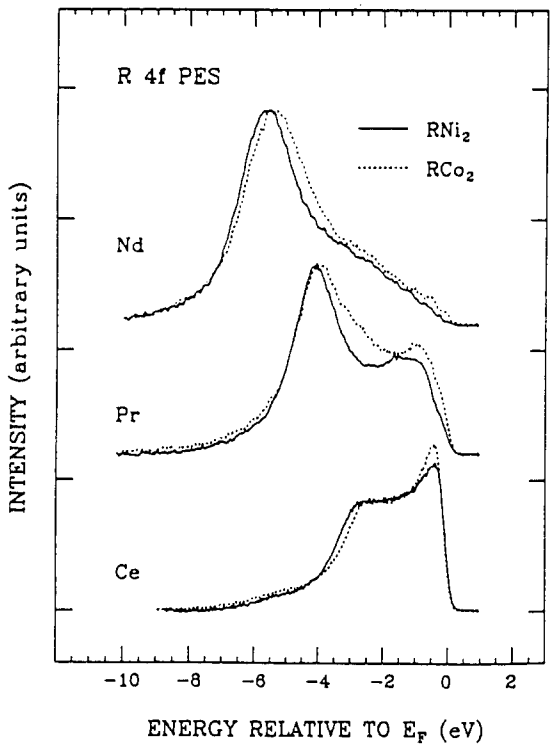

FIG. 1 Extracted R $4f$ PES spectra of RNi_2 (solid lines), in comparison to those of RCo_2 (dashed lines) with R = Ce, Pr, Nd (taken from Ref.[2]).

R=Ce to Pr and Nd.

(ii) The R$4f$/Ni$3d$ hybridization is smaller than the R$4f$/Co$3d$ hybridization.

In this paper, we evaluate explicitly the the R$4f$/T$3d$ hybridization matrix elements in RT_2 compounds to confirm the above speculation.

II. COMPUTATIONAL DETAILS

The magnitude of the R$4f$/T$3d$ hybridization could be estimated through an approach by Harrison and Straub [9]. This formalism combines the muffin-tin-orbital theory [10] with pseudo-potential concepts. A general hybridization matrix element is obtained through the second order coupling treatment, the result of which is given by

$$V_{ll'm} = (\eta_{ll'm}\hbar^2/m_e)\left[\left(r_l^{2l-1}r_{l'}^{2l'-1}\right)^{1/2}/d^{l+l'+1}\right]$$

$$\eta_{ll'm} = \frac{(-1)^{l'+1}}{6\pi}\frac{(l+l')!(2l)!(2l')!}{2^{l+l'}l!l'!}(-1)^m \times \left[\frac{(2l+1)!(2l'+1)!}{(l+m)!(l-m)!(l'+m)!(l'-m)!}\right]^{1/2}, \quad (1)$$

where l and l' are angular momentum quantum numbers of corresponding atoms ($l = 2$ for $3d-$ orbital of T atoms and $l = 3$ for $f-$ orbital of R atoms, respectively), m is the azimuthal quantum number, and m_e is the mass of an electron. Input parameters in the Eq.(1) are the characteristic lengths of the orbitals, $r_l, r_{l'}$, and the interatomic distance between R and T atoms, d. We have used the crystal structure data for the interatomic distance. RT_2 compounds crystallizes in $MgCu_2$- type $C15$ Laves phase structure with the space group $Fd3m$ [11]. The interatomic distance between R and T atoms is $\frac{\sqrt{11}}{8}a$, where a is the lattice constant. Spacing between R atoms occupying the Mg-sites and that between T atoms occupying the Cu-sites are equal to $\frac{\sqrt{3}}{4}a$ and $\frac{\sqrt{2}}{4}a$, respectively. In Fig.2, the lattice constants of RT_2 compounds are presented. Lattice constants of RCo_2 are larger than those of RNi_2 except for $CeCo_2$, while lattice constants of RFe_2 are largest.

The values of $r_l, r_{l'}$ characterize the average distances from the nuclei for each orbital. For r_l and $r_{l'}$, we have used the expectation values of the radial distances for the radial wave functions, R_l and $R_{l'}$, respectively. The radial wave functions are calculated by using ground state charge densities obtained from the linearized muffin-tin orbital (LMTO) band method within the local density approximation (LDA). In this calculation, all electrons are treated as core electrons.

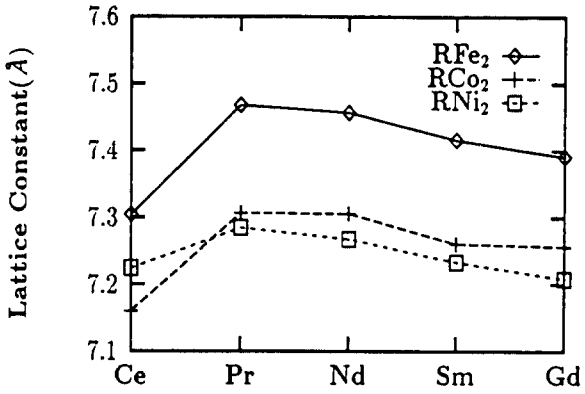

FIG. 2 Lattice constants of RT_2 compounds.

III. HYBRIDIZATION MATRIX ELEMENTS

In Fig.3, Radial probability density functions, $P_l(r) = 4\pi|rR_l(r)|^2$, are provided for $CeCo_2$ and $CeNi_2$. In this figure, one can see that $P_{3d}(r)$ of T atoms overlaps substantially with $P_{5d}(r)$, but little with $P_{4f}(r)$ of Ce atoms. Thus we expect that there would be a large hybridization between T$3d$ and Ce$5d$ states, and that Ce$4f$ states might interact with T$3d$ states via Ce$5d$ states (or via any other conduction electrons). This fact supports the validity of using the Harrison and Straub's formalism [9] for the evaluation of the hybridization matrix elements, which uses the second order coupling treatments are used.

Table 1 summarizes the calculated interatomic distances, d_{R-T}, average distances from the nuclei, r_d and r_{4f}, hybridization matrix elements, V_{df}, between R$4f$ and T$3d$ states for $m = 0$. Fig.4 exhibits the trend of V_{df} for RT_2 compounds. We have dropped the index m, since it is sufficient to consider only $\sigma-$ bonds to describe general trends. It is seen that the R$4f$/T$3d$ hybridization decreases as R becomes heavier, which implies that R$4f$ states become more localized with an increasing atomic

number. This is clearly seen in Table I, where the average distance of $4f$ orbital, r_f, decreases a lot as the atomic number of R atom increases. Consequently, the hybridization interaction of R $4f$/R $5d$-conduction electrons becomes reduced.

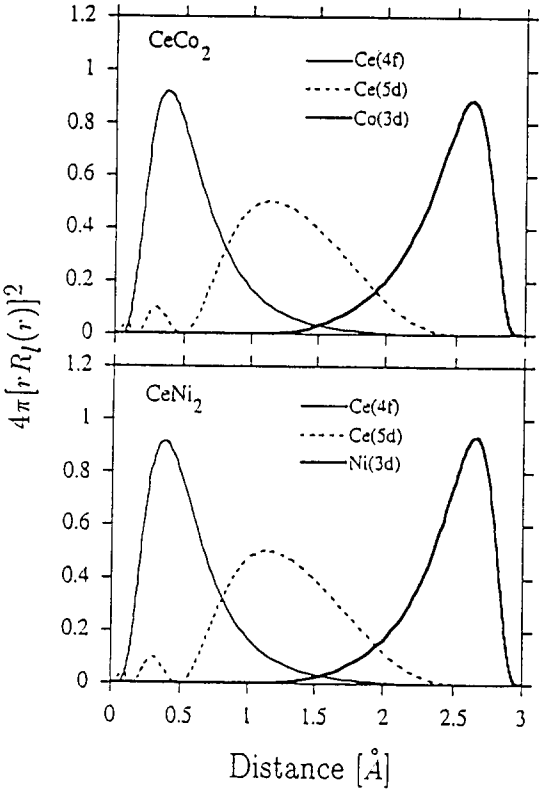

FIG. 3 Top : Radial probability density functions of $4\pi|rR_l|^2$ for Ce $4f$, for Ce $5d$, and Co $3d$ states, where R_l denotes a corresponding radial wave function for $CeCo_2$. Ce and Co atoms are separated by an amount corresponding to the interatomic distance. Bottom : Similarly for $CeNi_2$.

It is also notable that, despite smaller lattice constants of RNi_2 than those of RCo_2 (except for $CeNi_2$), the hybridizations in RNi_2 are smaller than in RCo_2 for a given R. This is contradictory to the expectation that the smaller lattice constant will yield a larger hybridization matrix element as indicated in Eq. (1). Furthermore, hybridization strengths in RFe_2 are comparable to those in RNi_2, although lattice constants of RFe_2 are much larger. These features can be understood from the fact that T $3d$

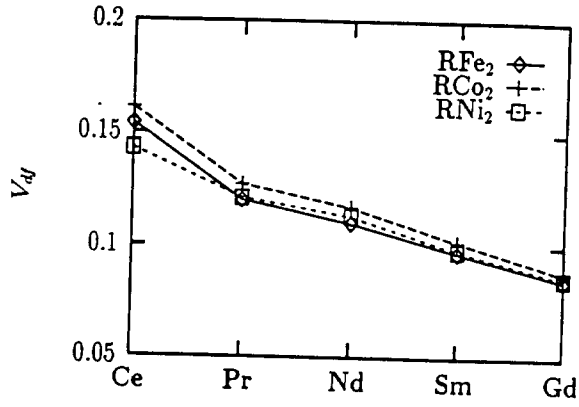

FIG. 4 The calculated hybridization matrix elements V_{df} of RFe_2 (solid lines), RCo_2 (dotted lines) and RNi_2 (dashed lines) compounds.

states become more localized as T goes from Fe to Co, Ni, as demonstrated in Table I. That is, the average distance of $3d$ orbital, r_d, decreases as the atomic number of T atom increases. Hence, a reduction of the hybridization due to the larger $R-T$ distance in a RFe_2 compound is compensated by an enhancement due to more delocalized nature of Fe $3d$ states. These trends are consistent with those found in R $4f$ spectra of RT_2 compounds (see Fig.1), i.e., that the hybridization of R $4f$ with conduction electrons decreases as R becomes heavier, or as T varies from Co to Ni.

TABLE 1. Crystal structure data of the $R-T$ distances, d_{R-T} [Å], calculated MTO radii of T $3d$, r_d [Å], and R $4f$, r_f [Å], and matrix elements, V_{df}[eV].

		d_{R-T}	r_d	r_f	V_{df}
RFe_2	$CeFe_2$	3.028	0.584	0.571	0.154
	$PrFe_2$	3.096	0.584	0.546	0.120
	$NdFe_2$	3.091	0.584	0.526	0.110
	$SmFe_2$	3.075	0.583	0.492	0.097
	$GdFe_2$	3.064	0.582	0.464	0.085
RCo_2	$CeCo_2$	2.969	0.557	0.572	0.161
	$PrCo_2$	3.031	0.557	0.546	0.127
	$NdCo_2$	3.026	0.556	0.526	0.117
	$SmCo_2$	3.010	0.556	0.492	0.102
	$GdCo_2$	3.009	0.555	0.464	0.088
RNi_2	$CeNi_2$	2.995	0.532	0.572	0.143
	$PrNi_2$	3.020	0.532	0.547	0.121
	$NdNi_2$	3.013	0.531	0.528	0.113
	$SmNi_2$	2.999	0.531	0.494	0.098
	$GdNi_2$	2.988	0.530	0.465	0.086

IV. CONCLUSION

By employing the muffin-tin-orbital theory combined with pseudo-potential concepts, hybridization matrix elements between different lattice sites are evaluated for RT_2 compounds (R:Ce, Pr, Nd, Sm, Gd; T=Fe, Co, Ni). It is found that the R $4f$/T $3d$ hybridization matrix elements decrease as R becomes heavier, which originates from the fact that R $4f$ states become more localized with an increasing atomic number. It is also found that the R $4f$/T $3d$ hybridization matrix elements are smaller in RNi_2 than in RCo_2. Further, the magnitudes of hybridization matrix elements in RFe_2 are found to be comparable to those in RNi_2, despite the larger lattice constants of RFe_2. These features indicate that the T $3d$ states become more localized as T goes from Fe to Co, Ni. The trends found in this work are consistent with those in recent PES experiments.

ACKNOWLEDGMENTS

This work was supported by the POSTECH-BSRI program of the Korean Ministry of Education and in part by the Korea Science Engineering Foundation through the SRC program of SNU-CTP.

REFERENCES

[1] J. -S. Kang, J. H. Hong, J. I. Jeong, S. D. Choi, C. J. Yang, Y. P. Lee, C. G. Olson, B. I. Min and J. W. Allen, Phys. Rev. B **46**, 15689 (1992).

[2] J. -S. Kang, J. H. Hong, J. I. Jeong, S. D. Choi, C. J. Yang, Y. P. Lee, C. G. Olson, Kicheon Kang and B. I. Min, Phys. Rev. B **49**, 16248 (1994).

[3] J. K. Lang, Y. Baer and P.A. Cox, J. Phys. F **11**, 121 (1981).

[4] O. Gunnarsson and K. Schoenhammer, Phys. Rev. B **28**, 4315 (1983) ; *ibid*, **31** 4815 (1985) ; in *Handbbok on the Physics and Chemistry of Rare Earths*, edited by K. A. Gschneidner, L. Eyring and S. Hüfner (North-Holland, Amsterdam, 1987), vol **10**, p.103.

[5] J. W. Allen, S. -J. Oh, O. Gunnarsson, K. Schoenhammer, M. B. Maple, M. S. Torikachvili and I. Lindau, *Adv. Phys.*, **35**, 275 (1987).

[6] M. R. Norman, D. D. Koelling, A. J. Freeman, H. J. F. Jansen, B. I. Min, T. Oguchi and L. Ye, Phys. Rev. Lett. **53**, 1673 (1984) ; A. J. Freeman, B. I. Min and M. R. Norman, in *Handbook on the Physics and Chemistry of Rare Earths*, edited by K. A. Gschneidner, L. Eyring and S. Hüfner (North-Holland, Amsterdam, 1987), vol **10**, p.165.

[7] D. W. Lynch and R. D. Cowan, Phys. Rev. B **36**, 9228 (1987).

[8] F. Gerken, A. S. Flodstrom, J. Barth, L. I. Johansson and C. Kunz, Phys. Scr. **32**, 43 (1985).

[9] W. A. Harrison, Phys. Rev. B **28**, 550 (1983) ; W. A. Harrison and G. K. Straub, Phys. Rev. B **36**, 2695 (1987).

[10] O. K. Andersen and O. Jepson, Physica B **91**, 317 (1977).

[11] *Crystallographic Data on Metal and Alloy Structures*, edited by A. Taylor and B. J. Kagle (Dover, New York, 1963).